

Gaseous Galactic Halos and QSO Absorption Line Systems

H.J. Mo

Max-Planck-Institut für Astrophysik, 85748 Garching, Germany

Abstract. Recent observations have shown that (some) metal line absorption systems in QSO spectra arise from gas in galactic halos with radii much larger than the optical radii of galaxies. We show that the observed galaxy-absorber connections are natural results of galaxy formation in hierarchical cosmogonies, where galaxies form from gas cooling and condensation in dark matter halos.

1. Introduction

There is now much evidence that metal line absorption systems in QSO spectra arise from gas in galactic halos. Recent imaging and spectroscopic observations can identify directly, at low redshift ($z \lesssim 1$), the galaxies associated with the MgII absorption systems (e.g. Bergeron, Cristiani, & Shaver 1992; Bechtold & Ellingson 1992; Steidel 1995; see Steidel 1998 for a recent review). The properties of such galaxy/absorber systems can be briefly summarized as follows: (i) Most MgII systems with rest-frame equivalent widths $W > 0.3\text{\AA}$ are associated with galaxies; (ii) Most galaxies with (K -band) luminosity $L_K \gtrsim 0.05L_K^*$ have gaseous halos to produce MgII systems with $W > 0.3\text{\AA}$; (iii) The typical absorption radius of a galaxy with $L_K \gtrsim 0.05L_K^*$ is $R_a \sim 35 h^{-1}\text{Kpc}(L_K/L_K^*)^{0.15}$, much larger than the optical radius; (iv) Galaxies with $L_K \lesssim 0.05L_K^*$ have much smaller absorption cross sections than the brighter ones; (v) For bright galaxies, the absorbing clouds has roughly spherical distribution, with a covering factor $\gtrsim 1$ within R_a , as indicated by the fact that few interlopers are observed; (vi) The absorbing galaxies show wide range of colors, from that of late type spirals to that of early type ellipticals, indicating that bright galaxies of all types possess similar gaseous halos; (vii) The observed absorption line systems show velocity structures, with typical velocity spread of $\sim 50\text{-}200\text{ km s}^{-1}$ (e.g. Petitjean & Bergeron 1990; Churchill 1998), consistent with the absorption clouds moving in the potential wells of galaxies; (viii) The absorbing gas is enriched, as heavy elements are observed.

Despite of the many observational facts about the relations between galaxies and the metal line absorption systems, relatively few theoretical work has been done. In particular, the importance of such observational results to our understanding of galaxy formation has not been fully explored.

In hierarchical clustering models of galaxy formation, it is assumed that galaxies form at the centers of dark matter halos as gas collapses, is shocked, and cools. Although our knowledge of how galaxies form is still incomplete at

present time, what is certain is that at some time in the past gas had to dissipate and move from the outer parts to the inner parts of the dark matter halos around galaxies, and in this process it must have produced absorption line systems in any quasar line-of-sight intercepting galactic halos. It is clear that in order to understand galaxy formation we must first understand the physical state of the gas out of which galaxies form, and that absorption line systems are an excellent observational probe to any gas dissipating in halos. Thus, the observational evidence that the high column density absorption systems at $z \lesssim 1$ indeed arise in gaseous halos around galaxies should be a landmark for our understanding of galaxy formation. Based on these considerations, we have proposed a simple two-phase model for the gaseous structure of galactic halos (see Mo, 1994; Mo & Miralda-Escudé 1996). The model is based on current scenario of galaxy formation in hierarchical clustering models, and so allows us to understand the absorption line systems in the general framework of structure formation in the universe. It was found that the observed galaxy-absorber connections are natural results of galaxy formation in hierarchical cosmogonies.

2. The Structure of Gaseous Galactic Halos

During the process of galaxy formation, intergalactic gas collapse and move inward through the extended dark matter halos that are observed around present galaxies. A halo of hot gas at the virial temperature will form as the kinetic energy of the infalling material is thermalized in shocks. In low mass halos, the cooling time of this hot halo gas is short compared to the dynamical time if it contains all the accreted baryons; therefore, the gas must cool until the density of hot gas decreases to a level such that the cooling time is similar to the age of the system. Due to the increased cooling rate as temperatures drop, a two-phase medium will naturally form in these conditions of rapid cooling. Clouds photoionized by a radiation background will be maintained at an equilibrium temperature of about 10^4 Kelvin, in pressure equilibrium with the hotter halo gas. These clouds could form from inhomogeneities in the halo gas, or from the ram-pressure stripped interstellar medium of satellite galaxies. Due to their higher density, clouds will fall to the center of the halo where they may form globular clusters or settle into gaseous disks. In such a scenario, modeling the structure of gaseous galactic halos involves both the formation of dark matter halos and the state of gas in dark matter halos. The following is a sketch of the main ingredients involved in such a modeling.

2.1. Dark halos

The properties of dark matter halos in hierarchical clustering cosmogonies [such as cold dark matter (CDM) models] are relatively well understood from analytic models and N-body simulations. Dark matter halos can be described roughly as singular isothermal spheres, with density profiles given by

$$\rho(r) = \frac{V_c^2}{4\pi G r^2}; \quad V_c = \left(\frac{GM}{r_v} \right)^{1/2}. \quad (1)$$

where V_c is the circular velocity, M is the mass, and r_v is the virial radius, of the halo. From spherical collapse model, the virial radius can be defined as $r_v = V_c/10H(z)$, where $H(z)$ is the Hubble constant at redshift z .

For a given cosmogonic model, one can also estimate the mass function of dark matter halos, $n(M; z)dM$, which gives the comoving number density of dark matter halos, with mass in the range $M \rightarrow M + dM$, at a given redshift z . This function can be estimated either from N-body simulations, or from analytic models such as the Press-Schechter formalism. Thus, the number of halos which may host absorption line systems can be obtained.

As demonstration, results in the following are shown only for the standard CDM cosmogony with $\Omega_0 = 1$, $h = 0.5$, and $\sigma_8 = 0.67$.

2.2. Gas in Dark Matter Halos

Before the collapse of a dark matter halo, gas on a mass shell moves together with dark matter particles until the velocity of the mass shell reaches the sound speed of the gas interior to the mass shell, where the gas is shocked while dark matter particles continue to collapse and virialize. Analytic models (e.g. Bertchinger 1989) and numerical simulations (e.g. Evrard 1990) show that, if cooling is not efficient then the gas in a dark halo will be shock-heated to the virial temperature

$$T_v = \mu \frac{V_c^2}{2k}, \quad (2)$$

with a profile similar to that of the dark halo. Because the gas density is higher near the center of a halo, radiative cooling of the gas is more efficient there. We define a cooling radius r_c by

$$f\rho(r_c) = \frac{5\mu k T_v}{2\Lambda(T_v)t_M}, \quad (3)$$

where $\Lambda(T)$ is the cooling rate, μ is the average mass per particle, f is the gas mass fraction and $t_M \sim t/2$ is the time between major mergers. Thus, gas located at $r \ll r_c$ can cool effectively before the halo merges into a larger system, while that at $r \gg r_c$ cannot cool and should retain its original state. Based on this consideration, we model the density profile of the hot component as

$$\rho_{\text{hot}}(r) = \frac{fV_c^2}{4\pi Gr(r+r_c)}, \quad (4)$$

so that $\rho_{\text{hot}}(r) \rightarrow f\rho(r)$ for $r \gg r_c$ and $\rho_{\text{hot}}(r) \propto 1/r$ for $r \ll r_c$. The temperature of this phase is assumed to be at $T_{\text{hot}} \sim T_v$. These behaviours of $\rho_{\text{hot}}(r)$ are similar to those obtained from the self-similarity solution given by Bertchinger (1989). When $r_c > r_v$, the cooling time at the virial radius is already short compared to t_M . In this case we assume $r_c = r_v$.

The accreted gas that does not stay in the hot phase and cools must fall through the hot halo in the form of photoionized clouds. We refer to the gas in these clouds as the ‘‘cold phase’’. The rate at which cold gas accumulates in a halo is determined by both gas infall and gas cooling, and is roughly

$$\dot{M}_{\text{cold}} \sim \frac{fV_c^2}{Gt_M} r_{\text{min}}; \quad r_{\text{min}} = \min[r_v, r_c]. \quad (5)$$

We assume the mass flow rate to be $\dot{M} = M/t_M$, and that the clouds move to the halo center with a constant velocity v . Assuming also spherical symmetry for the gas distribution, we can write the density of the cold gas as a function of the distance r to the halo center as

$$\rho_{\text{cold}}(r) = \frac{\dot{M}}{4\pi r^2 v}. \quad (6)$$

In the absence of a hot phase, the cold gas is in free fall and v must be of the order of the virial velocity V_c . The friction of hot gas may cause cold clouds to move at a terminal velocity which is smaller than V_c . However, since halos on galactic scales have cooling times that are similar to the dynamical times, the inflow velocity should not be much smaller than the virial velocity. This is also consistent with the observed velocity structure in MgII systems. The cold clouds are assumed to be at a temperature $T_{\text{cloud}} \sim 10^4\text{K}$, they are also assumed to be in pressure equilibrium with the hot gas, so that the density of a cloud (assumed to be uniform) at a radius r is

$$\rho_{\text{cloud}} \sim \rho_{\text{hot}}(r) T_{\text{hot}}/T_{\text{cloud}}. \quad (7)$$

2.3. Cloud properties

In the model outlined above, cold clouds are moving in diffuse substrates of hot gas. Various physical processes can act to affect the formation and destruction of the clouds. These processes constrain the masses and densities of the clouds. When the mass of a cloud is too large and its density too high, the cloud will become gravitationally unstable as it sinks towards the halo center. This happens when the cloud mass exceeds the Jeans mass. Once a cloud is accelerated to a terminal velocity at which the drag force of the hot medium is comparable to the self-gravitating force on its surface, the cloud may become hydrodynamically unstable. Small clouds are also unstable against heat conduction. Based on these considerations, we found that the masses of cold clouds are confined to a narrow range, $M_{\text{cloud}} \sim 10^6 M_{\odot}$. The typical size of such a cloud is $\sim 1\text{Kpc}$. The covering factor of such clouds is ~ 1 within $\sim 30 h^{-1}\text{Kpc}$ for halos with $V_c \sim 200\text{ km s}^{-1}$.

3. Implication for QSO Absorption Line Systems

To make connections between gaseous halos and QSO absorption line systems, we need to calculate the column densities of ions (of some species) at different impact parameters from a halo. We assume that the gas is ionized by the UV background radiation with a flux $J(\nu)$ which we parameterize as

$$J(\nu) = J_{-21}(z) \times 10^{-21} \left(\frac{\nu}{\nu_{\text{HI}}} \right)^{-\alpha} \Theta(\nu) \text{ erg cm}^{-2} \text{ sr}^{-1} \text{ hz}^{-1} \text{ sec}^{-1}, \quad (8)$$

where ν_{HI} is the hydrogen Lyman limit frequency, $J_{-21}(z)$ gives the redshift dependence of $J(\nu)$, and $\Theta(\nu)$ describes departures of the spectrum from a power-law. A typical spectrum can be represented approximately by taking $\alpha = 0.5$, $J_{-21}(z) = 0.5$ for $z > 2$ and $J_{-21}(z) = 0.5 \times [(1+z)/3]^2$ for $z < 2$, and

including a break in the spectrum at $\nu_4 \equiv 4$ Ryd (due to continuum absorption by HeII), with $\Theta(\nu < \nu_4) = 1$ and $\Theta_4 \equiv \Theta(\nu \geq \nu_4) = 0.1$.

To consider metal line systems, we also need to assume a metallicity, Z , of the gas. The exact level of chemical enrichment in galactic halos is not clear. In the disk-spheroid model of our Galaxy, the metal output from stars in the spheroid component can enrich the disk gas to a level of about $0.2Z_\odot$ (see Binney & Tremaine 1987, §9.2). In this model, the gas in the halo was initially enriched to such a level before it settles into the disk. In the galaxy formation model of White & Frenk (1991), gas in halos with $V_c \gtrsim 100 \text{ km s}^{-1}$ could also be enriched to a level of 0.1-0.3 Z_\odot (see their Fig. 4), because of star formation in the progenitors and that in halos themselves. Unfortunately, the detail result depends crucially on how well the output metal is mixed with halo gas. In our model we treat Z as a free parameter.

With this assumptions, the number density of any species of ions can be obtained as a function of the radius from the center of a halo with circular velocity V_c at redshift z . As a result, for single halos we can obtain $N_X(D)$, the column density of species X expected at an impact parameter D , and $D(N_X)$, the impact parameter at which the column density is N_X . Given the number density of dark halos as a function of V_c and z (e.g. from the Press-Schechter formalism), we can also obtain the statistical properties of absorption systems.

The left panel of Figure 1 shows the HI column density N_{HI} versus impact parameters for halos at $z = 0.5$ with various V_c . The value of z chosen here is to match the mean redshift of the MgII systems for which associated galaxies are identified (e.g. Steidel 1995). As one can see, N_{HI} decrease with D . This is because N_{HI} is proportional to the total column density of cold gas, which is higher for a smaller impact parameter, and to the pressure (since neutral fraction increases with pressure), which is higher near the center. The figure shows that the impact parameter for producing a Lyman limit system (LLS) with $N_{\text{HI}} \gtrsim 10^{17} \text{ cm}^{-2}$ is about $40 h^{-1} \text{ Kpc}$ at $V_c \sim 200 \text{ km s}^{-1}$. In halos with $V_c \gtrsim 250 \text{ km s}^{-1}$, this impact parameter is not much larger because the cooling radius is reached, and we assume that no clouds are formed outside r_c .

The shape of the MgII column density profile (shown in the right panel of Fig.1) is similar to that of HI, because $N_{\text{MgII}}/N_{\text{HI}}$ is roughly a constant for the photoionization model considered here. The observed samples of MgII absorption lines select systems where the MgII line is above a threshold of equivalent width. We present results for the number of absorbers and the impact parameter distribution assuming a fixed threshold $N_{\text{MgII}} = 2 \times 10^{13} \text{ cm}^{-2}$ (reasonable for $W = 0.3 \text{ \AA}$), although we should bear in mind that the average cloud covering factor can also affect the observed equivalent widths. The left panel of Figure 2 shows the results for the impact parameter in halos of different V_c , at redshift $z = 0.5$. The UV flux spectrum used here has parameters $J_{-21} = 0.1$, $\alpha = 0.5$ and $\Theta(\nu \geq \nu_4) = 0.1$. At $V_c \lesssim 150 \text{ km s}^{-1}$, D decreases rapidly with decreasing V_c , due to the faster cooling rate and the lower pressures that are implied. The typical impact parameter is about $30 h^{-1} \text{ Kpc}$ at $V_c \sim 200 \text{ km s}^{-1}$. In halos with $V_c \gtrsim 250 \text{ km s}^{-1}$, this impact parameter is not much larger again because the cooling radius is reached and no clouds are assumed to form outside the cooling radius. This result of impact parameter as a function of V_c is similar to the observational result of Steidel et al. (see Steidel 1995). The observation shows

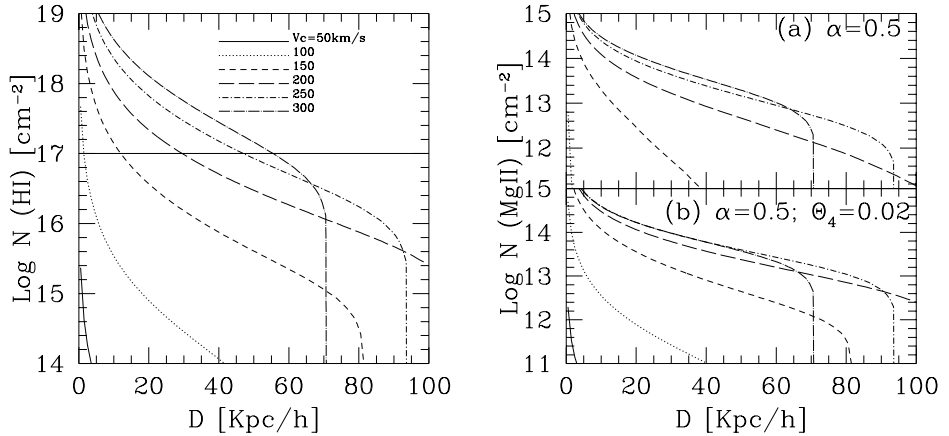


Figure 1. **Left panel:** HI column density as a function of impact parameter D , for halos at $z = 0.5$ and with various V_c . The model parameters are $f = 0.05$, $Z = 0.3Z_\odot$ and $v = V_c$. The horizontal line indicates $N_{\text{HI}} = 10^{17} \text{ cm}^{-2}$, above which an LLS is produced. **Right panel:** MgII column density as a function D . Results are shown for two models of UV flux, one is a power law with power index $\alpha = 0.5$, the other has the same power index but with a break at 4 Ryd so that $\Theta_4 \equiv \Theta(\nu \geq \nu_4) = 0.02$. In both cases $J_{-21} = 0.1$.

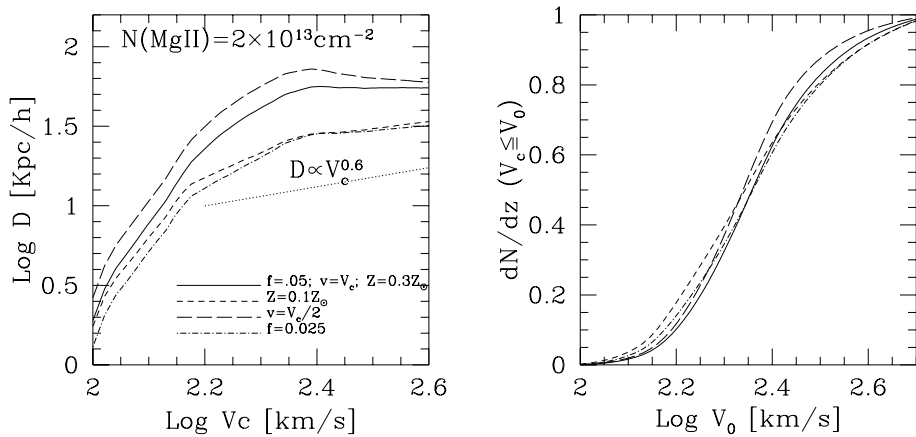


Figure 2. **Left panel:** The impact parameter D , at which $N_{\text{MgII}} = 2 \times 10^{13} \text{ cm}^{-2}$, as a function of halo circular velocity. Results are shown for halos at $z = 0.5$. The dotted line shows the relation $D \propto V_c^{0.6}$. **Right panel:** Cumulative cross section of MgII systems at $z = 0.5$, with $N_{\text{MgII}} \geq 2 \times 10^{13} \text{ cm}^{-2}$, given by halos with circular velocity $V_c \geq V_0$, as a function of V_0 .

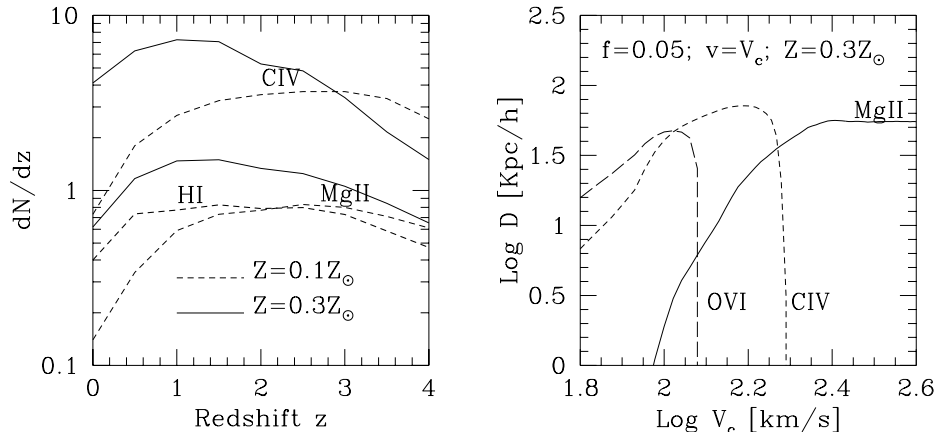


Figure 3. **Left panel:** Number of absorption systems per unit redshift, for HI systems with $N_{\text{HI}} \geq 10^{17} \text{cm}^{-2}$, MgII systems with $N_{\text{MgII}} \geq 2 \times 10^{13} \text{cm}^{-2}$, and CIV systems with $N_{\text{CIV}} \geq 10^{14} \text{cm}^{-2}$. Solid curves assume $f = 0.05$ and $v = V_c$ with $Z = 0.3Z_{\odot}$; dashed curves assume the same f and v but with $Z = 0.1Z_{\odot}$. **Right panel:** The impact parameters at which $N_{\text{MgII}} = 2 \times 10^{13} \text{cm}^{-2}$ (solid), $N_{\text{CIV}} = 10^{14} \text{cm}^{-2}$ (short dashed), and $N_{\text{OVI}} = 10^{14} \text{cm}^{-2}$ (long dashed), as a function of V_c for halos at $z = 0.5$.

that the maximum impact parameter D of their MgII systems to the absorbing galaxies (having typically $L_K \gtrsim 0.05L_K^*$) increases slowly with the K-band luminosity L_K as $D \propto L_K^{0.15}$. Assuming the Tully-Fisher relation $L_K \propto V_c^4$, we have $D \propto V_c^{0.6}$, which is shown in the left panel of Fig.2 by the dotted line. We see that such a weak increase of D with V_c can be accommodated in our model, arising from the value of the cooling radius and the derived gas pressures in different halos. The very small impact parameters in low V_c halos agrees with the fact that MgII absorption systems are not commonly found in galaxies fainter than about $0.1L^*$ (Steidel 1995).

To see how different halos contribute to the MgII absorption, we plot in the right panel of Fig.2 the cumulative number of MgII systems per unit redshift at $z = 0.5$, produced in halos with $V_c \leq V_0$. The figure shows that most MgII systems are produced in halos with $V_c = 150\text{-}300 \text{km s}^{-1}$. The median V_c is about 200km s^{-1} . The contribution to the total cross section made by halos with $V_c \lesssim 150 \text{km s}^{-1}$ is small, which again suggests that MgII systems should not be commonly found in the halos of dwarf galaxies.

The left panel in Fig.3 shows the total number of MgII systems and the evolution with redshift, compared to the number of LLSs, for two values of the metallicity. The relative number of MgII systems to LLSs is correctly predicted when the metallicity is between $Z = 0.1\text{-}0.3$, (compared with the observational results in Steidel & Sargent 1992), and the evolution is also as observed if the metallicity in these halo clouds does not decrease very fast with redshift. For

comparison, the total number of CIV systems in our model is also shown in the panel; the ratio to the number of MgII systems, and the evolution with redshift, is similar to what is observed. Fig.3 (right panel) also compares the impact parameters of CIV systems with those of MgII systems in different halos. In small halos, D is much larger for CIV systems than for MgII systems. In fact, the cross-section weighted average of V_c is only about 100 km s^{-1} for the CIV systems, but as large as about 200 km s^{-1} for MgII systems, in the standard CDM model considered here. Our model thus predicts that, while MgII systems are mostly associated with bright galaxies, many CIV systems should be found to be associated with small galaxies where N_{MgII} is low. For the same reason, OVI systems should neither be commonly found as photoionized clouds in halos with $V_c \gtrsim 150 \text{ km s}^{-1}$. Some of such highly-ionized systems may arise from collisionally ionized gas (e.g. in the hot phase) or from an intermediate temperature phase between the hot medium and the cold clouds.

4. Discussion

We have demonstrated that the simple halo model discussed in §2 can indeed reproduce the main properties of the observed galaxy-absorber connections. This is important, because it means that the observed absorption systems can be understood in the current framework of galaxy formation. Much theoretical work remains to be done to see the plausibility of our model and to make it more predictive, mainly to understand the physical processes determining the rate of formation and destruction of gas clouds moving through the halo, the distribution of cloud masses and velocities, etc. Further observations of absorption line systems and their relation to galaxies should open a new era in our understanding of how galaxies form, as the physical conditions of the gas in the halos around galaxies, and the dependence of these conditions on galaxy luminosity and morphology are unravelled.

References

- Bechtold J., Ellingson E., 1992, ApJ, 396, 20
 Bertchinger E., 1989, ApJ, 340, 666
 Bergeron J., Cristiani S., Shaver P., 1992, A&A, 257, 417
 Binney J., Tremaine S., 1987, Galactic Dynamics, Princeton Univ. Press
 Churchill C., 1998, this volume
 Evrard A.E., 1990, ApJ, 363, 349
 Mo H.J., 1994, MNRAS, 269, L49
 Mo H.J., Miralda-Escudé J., 1994, ApJ, 430, L25
 Petitjean P., Bergeron J., 1990, A&A, 231, 309
 Steidel C.C., 1995, in QSO Absorption Lines, ed. G. Meylan, Springer, p.137
 Steidel C.C., 1998, this volume
 Steidel C.C., Sargent W.L.W., 1992, ApJS, 80, 1
 White S.D.M., Frenk C., 1991, ApJ, 379, 52